Journal of Alloys and Compounds 910 (2022) 164903

Contents lists available at ScienceDirect

Journal of Alloys and Compounds

journal homepage: www.elsevier.com/locate/jalcom

Photoelectron-induced quantitative regulation of ferromagnetism in Permalloy at room temperature for photovoltaic flexible spintronics

Wanjun Peng[a], Lei Wang[b,*], Yaojin Li[a], Yujing Du[a], Zhexi He[a], Chenying Wang[c], Yifan Zhao[a,c,**], Zhuangde Jiang[a,c], Ziyao Zhou[a,c], Ming Liu[a,c]

[a] Electronic Materials Research Laboratory, Key Laboratory of the Ministry of Education & International Center for Dielectric Research, School of Electronic Science and Engineering, State Key Laboratory for Manufacturing Systems Engineering, Collaborative Innovation Center of High-End Manufacturing Equipment, Xi'an Jiaotong University, Xi'an 710049, China
[b] Center for Spintronics and Quantum Systems, State Key Laboratory for Mechanical Behavior of Materials, Xi'an Jiaotong University, Xi'an 710049, China
[c] The International Joint Laboratory for Micro/Nano Manufacturing and Measurement Technology, Xi'an Jiaotong University, Xi'an 710049, China

ARTICLE INFO

Article history:
Received 3 February 2022
Received in revised form 1 April 2022
Accepted 4 April 2022
Available online 6 April 2022

Keywords:
Interface charge doping
Magnetic anisotropy
Multiferroic heterostructure
Magnetoelectric coupling
Ferromagnetic resonance

ABSTRACT

Flexible spintronics has recently sparked an upsurge due to the growing demand for miniaturization, high-speed, integration and energy-saving in portable and wearable devices. However, the stress/strain during the substrate deformation process is inevitable for flexible spintronic devices and may be available to assist the switching of the magnetization, accordingly. Therefore, combined with the previously discovered high energy efficient sunlight controlled magnetization switching, we propose a bending-insensitive photovoltaic flexible spintronic device constructed by PET/Ta/Permalloy/($PC_{71}BM$: PTB7-Th)/Pt heterostructure. The bent device achieved a 281 Oe of maximal ferromagnetic resonance (FMR) field shift by photoelectrons in a reversible manner under the sunlight soaking at room temperature. And the magnetic change as a function of the external light radiation was precisely determined. These findings provide a feasible way to combine the flexible substrate and photoelectrons for energy-saving and precise manipulation of magnetism in bendable spintronic devices.

1. Introduction

In the emerging mobile internet era, the microelectronics and information technology industry depend on flexible spintronics that exploits the spin and charge of electrons based on flexible substrates, materials, or microstructures [1–6]. Just like the evolution from electricity to electronics, the transitions from solid spintronics to flexible spintronics make a great scientific and commercial impact [4,7–9]. To date, researchers have a growing motivation to fabricate flexible nano-films, a rapidly developing emerging high-tech industry. Permalloy (Py: $Ni_{80}Fe_{20}$) thin films are proved to be a good candidate for flexible devices, which benefits from the excellent high-frequency microwave characteristics such as high saturation magnetization (M_s), low coercivity field (H_c) and high Curie temperature (T_c), especially near zero magnetostriction coefficient permitting the magnetic properties insensitive to the bending [10,11]. It has been reported that Py based flexible devices have little strain-induced magnetic change and outstanding ductility under appropriate bending radius, which helps to promote the controllability, steady the whole structure conformal and increase tolerance of deformation [2,12]. These features make Py become an appropriate candidate for wearable/flexible electronics thereby.

It is well known that the regulation of magnetism plays an essential role in spintronics [13–17]. Researchers have sought several core ways that have been optimized to modulate the magnetism in spintronic devices for industrial application, including mechanical strain, electric field, thermal cycling and electric current.[18–37] However, the above methods still have some drawbacks with flexible the substrate for practical applications. The purely strain-tunable method will raise the issues of reduced durability and magnetic tuning under constant mechanical deformation. For the charge-mediated manipulation *via* ionic liquid, long response time and interfacial corrosion shrink the scope of applications. Moreover, the

* Corresponding author.
** Corresponding author at: Electronic Materials Research Laboratory, Key Laboratory of the Ministry of Education & International Center for Dielectric Research, School of Electronic Science and Engineering, State Key Laboratory for Manufacturing Systems Engineering, Collaborative Innovation Center of High-End Manufacturing Equipment, Xi'an Jiaotong University, Xi'an 710049, China.
E-mail addresses: wanglei.icer@xjtu.edu.cn (L. Wang), zhaoyifan100@xjtu.edu.cn (Y. Zhao).

https://doi.org/10.1016/j.jallcom.2022.164903
0925-8388/

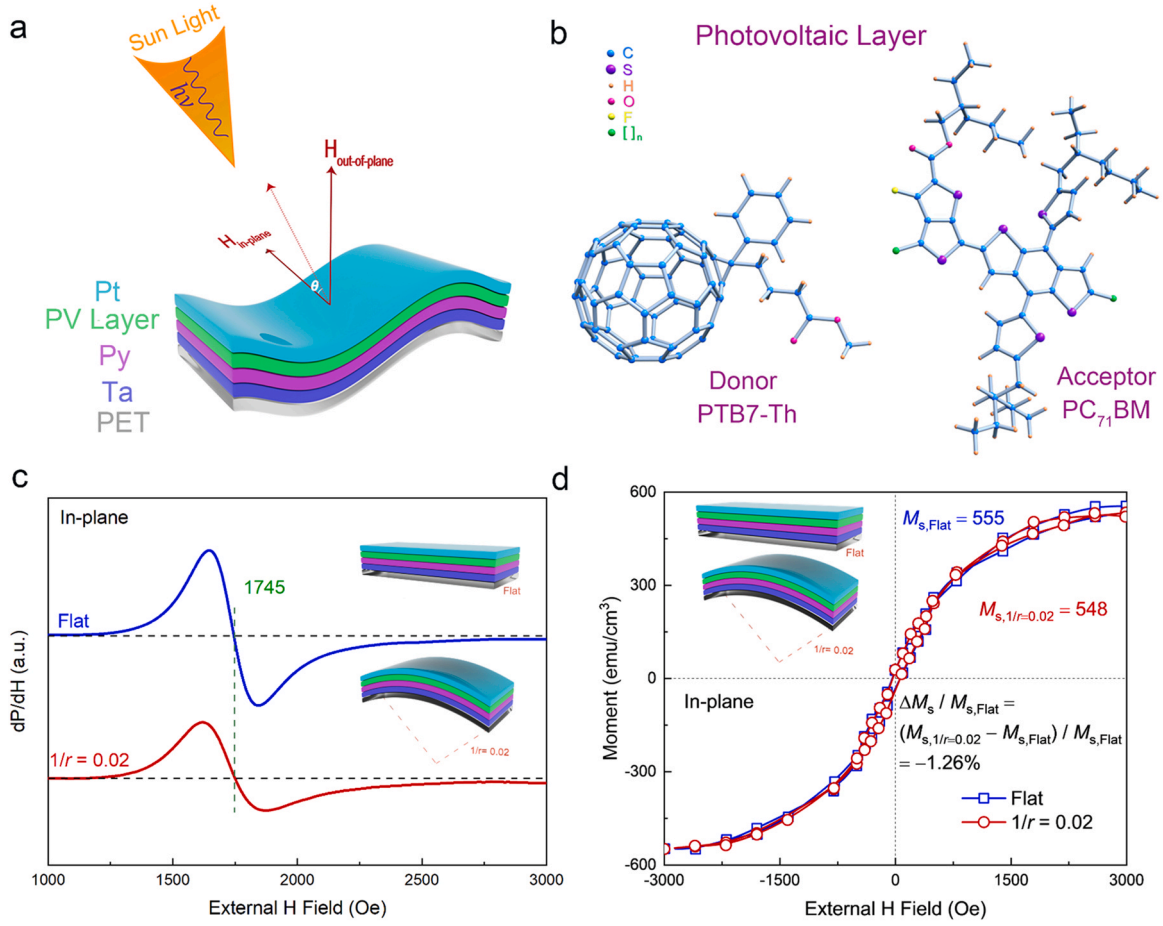

Fig. 1. Schematics of the flexible spintronics. (a) The PET/Ta/Permalloy/($PC_{71}BM$: PTB7-Th)/Pt flexible heterostructure. (b) The molecular structure of the donor (PTB7-Th) and acceptor ($PC_{71}BM$). The magnetism is unchanged with the substrate deformation from the initial flat state (blue line) to the bending state (red line) along the in-plane direction, observed *via in situ* (c) ESR and (d) VSM measurements.

conformality problems caused by thermal cycling-induced deformation and electric current-induced Joule heat limit the further improvement. On the other hand, the most widely used optical manipulation method is the femtosecond laser. Still, it is difficult to integrate for miniaturization, with high thermal effects and high-cost issues [38]. Therefore, the emergent methods for magnetic controlling based on flexible spintronics are still necessary to promote the utilization in the future.

In this work, we reported on the fabrication and characterization of a sunlight-controlled magnetic anisotropy within a polyethylene terephthalate (PET) substrate-based Ta/Py/($PC_{71}BM$: PTB7-Th)/Pt bendable heterostructure, as illustrated in Fig. 1a and b, respectively. Sunlight is considered to be a free energy source because it is ubiquitous. The chemical formulae of two organic photovoltaic materials are poly[4,8-bis(5-(2-ethylhexyl) thiophen-2-yl) benzo [1,2-b:4,5-b′] dithiophene-co-3-fluorothieno [3,4-b] thiophene-2-carboxylate] (PTB7-Th) and [6,6]-phenyl C_{71} butyric acid methyl ester ($PC_{71}BM$), respectively, which have been proved to be one of the most successful photovoltaic systems [39] (Fig. 1b). The *in situ* electron spin resonance spectroscopy (ESR) was conducted to quantitatively record magnetic anisotropy changes in the sunlight soaking at room temperature (RT). About 228 Oe and 281 Oe reversible FMR field shifts have been achieved under AM 1.5 G illumination at 100 mW/cm^2 (1 standard sun) with bending curvature $1/r = 0$ and 0.02 mm^{-1}, respectively. At the same time *in situ* vibrating sample magnetometry (VSM) measurements were utilized to further evidence the photon-induced magnetic anisotropy and magnetization changes ($\Delta M_s = -13.14\%$ with light irradiation). In addition, the heat resulting from sunlight induced FMR field variation has been excluded, proving that the PET/Ta/Py/($PC_{71}BM$: PTB7-Th)/Pt heterojunction is a desirable platform for wearable/flexible spintronic devices because the univariate regulation of magnetism has been realized. Meanwhile, the relationships between the light intensity and the magnetic anisotropy variations were also expounded. Finally, the first-principles calculation revealed that the photo-induced electrons doping in the Py film shifted the Fermi level of this ferromagnetic film and weakened the magnetization accordingly. Our findings may provide a solution for efficient, energy-saving, easily-integrated and precisely controllable flexible spintronic devices.

2. Results and discussion

The *in situ* ESR measurement is utilized to evaluate the bending induced magnetic anisotropy change of Py films, and the characterization method is according to our previous work [38]. In general, in-plane (IP) is defined such that the angle between the external magnetic field and the laminates films is 0°. Similarly, out-of-plane (OP) is defined such that the external magnetic field is perpendicular to the membrane surface. As shown in Fig. 1c, with curvature radius $r = 50$ mm ($1/r = 0.02$ mm^{-1}), corresponding to a strain $\varepsilon = -t/2r = 0.1\%$, where t is the thickness of the flexible PET, the value of FMR field (H_r) in the in-plane direction remains nearly constant, implying excellent deformation stability between the as-grown heterostructure and the flexible substrate. The *in situ* VSM measurement is conducted to further investigate the effect of

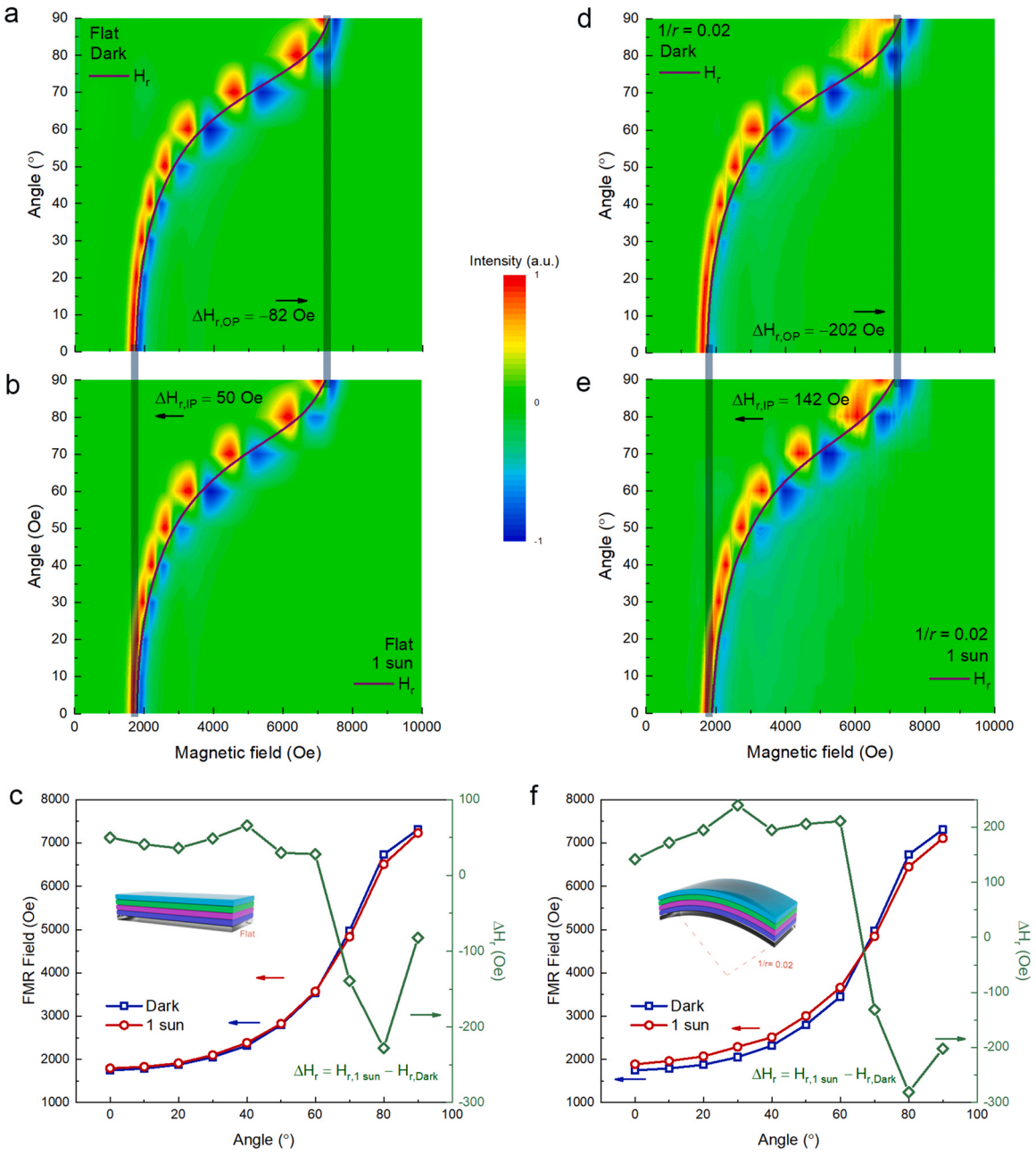

Fig. 2. Photovoltaic control of the magnetic anisotropy in the PET/Ta/Permalloy/($PC_{71}BM$: PTB7-Th)/Pt sandwich heterostructure. (a, b, d, e) Angular dependence of the sunlight tuning FMR phase diagram in the flat and bent state, respectively. The color scale shows the amplitude of the FMR absorption spectra. The purple line represents the positions of H_r. (c, f) The angular dependence of the FMR field observed by *in situ* ESR. The blue, red and green lines stand for the dark state, 1 sun state, and the FMR field change induced by the photovoltaic effect, which is measured with (c) flat condition and (f) bending state, respectively. The inset shows the schematic diagram of the photovoltaic device under a flat state or bending state.

bending conditions on the magnetic property change of magnetization. Fig. 1d shows that as the curvature increases from $1/r = 0$ to 0.02 mm^{-1}, the saturation magnetization (M_s) keeps almost invariant. Here, $M_{s,flat} = 555$ emu/cm^3 represents the M_s without any bending, and $M_{s,1/r=0.02} = 548$ emu/cm^3 is the M_s with the curvature $1/r = 0.02$ mm^{-1}. Besides, the variations of the H_r and M_s along the out-of-plane direction are also characterized with the same tendency, as shown in Fig. S1. Therefore, all the following characterization in this work will adopt the bending conditions of $1/r = 0$, $0.02 mm^{-1}$ in order to eliminate stress effects for the precise regulation of magnetism in flexible spintronic devices. Furthermore, the curvature ($1/r = 0.02 mm^{-1}$) is more in line with the radian of the human body surface, which is more conducive to meeting the practical requirements of wearable devices.

The sunlight-induced magnetic anisotropy variation is *in situ* characterized with the ESR, as illustrated in Fig. 2. The microwave response frequency can be tuned, proving the great potential in tunable RF/microwave device. Fig. 2a, b, d, e present the contour plots of angular-dependent sunlight tuning FMR spectra under flat and bent states at room temperature. The *x*-axis represents the magnetic field, while the *y*-axis shows the angle (θ) between the external magnetic field and the film plane. And the color map displays the FMR signal amplitude. Fig. 2c, f show the angular dependence of the photo-tuning FMR field. It can be seen that the in-plane direction is parallel to the easy axis because the minimum H_r is along with the magnetic layer. Correspondingly, the out-of-plane direction means the hard axis due to the maximum H_r. The standard sunlight intensity is AM 1.5 G at 100 mW/cm^2 (1 sun), which may have the

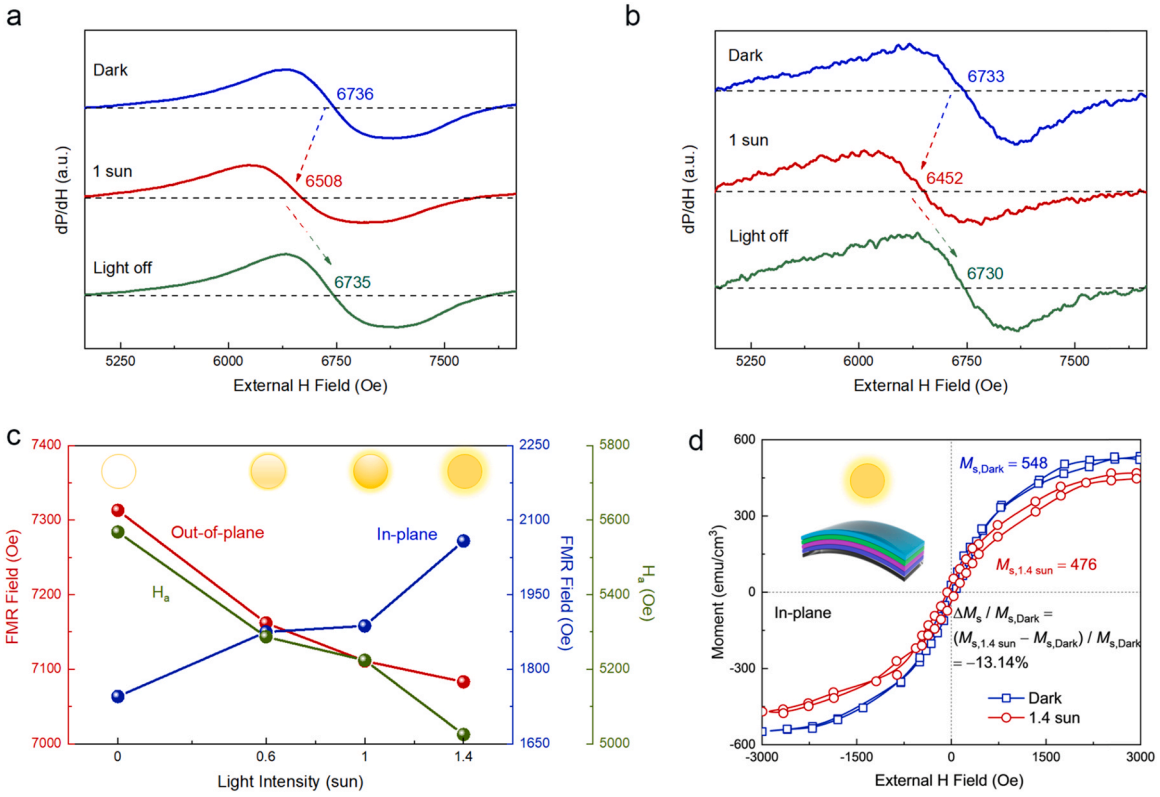

Fig. 3. (a, b) 1 sun visible light induced FMR field change from the initial dark state (blue line) to the excited state (red line) and then returned (green line) when the light source is removed, which are measured at 80° with (a) flat condition and (b) bending state, respectively. (c) FMR field and magnetic anisotropy H_a as a function of the light intensity at the bending state along with IP and OP, respectively. (d) The photovoltaic effect induced magnetic hysteresis loops variation along the in-plane direction at the bending state.

most common application scenarios. When applying 1 sun intensity of sunlight illumination, as shown in Fig. 2a-c, upward shifts of H_r are detected at $\theta = 0°$~$60°$, while downward variations are observed at $\theta = 70°$~$90°$ in a flat condition. In other words, the sunlight decreases the out-of-plane FMR field ($H_{r,OP}$) and increases the in-plane FMR field ($H_{r,IP}$), indicating that the magnetic anisotropy of Py films is weakening. Meanwhile, a similar tendency of the FMR field with curvature radius $1/r = 0.02$ mm^{-1} is also confirmed in Fig. 2d-f. The change of H_r under bending is more remarkable compared with the flat condition, demonstrating a better optical-electro-magnetic coupling effect in the bent state. The corresponding $\Delta H_{r,\ max}$ is −281 Oe and −228 Oe at $\theta = 80°$, respectively. As a function of magnetic anisotropy, the change of H_r can be described by the well-known Kittel equation:

$$f = \gamma\sqrt{(H_r + H_{eff})(H_r + H_{eff} + 4\pi M_s)} \quad (\text{in} - \text{plane}) \tag{1}$$

$$f = \gamma(H_r + H_{eff} - 4\pi M_s)(\text{out} - \text{of} - \text{plane}) \tag{2}$$

where f is the frequency of the microwave in the cavity, γ is the gyromagnetic ratio, $4\pi M_s$ is the saturation magnetization of Py, and H_{eff} is the effective magnetic field which can be influenced by sunlight illumination and strain/stress force [40–43]. From Fig. 1c and d above, strain-induced H_{eff} can be ignored at flat state without sunlight. Similarly, small H_{eff} is realized by sunlight illumination at flat state, as shown in Fig. 2a-c. However, enhanced H_{eff} with both sunlight and strain/stress conditions can be observed in Fig. 2d-f. This phenomenon deduces that optical-electro-magnetic coupling can be amplified at bending state, leading to a larger shift in H_r, which is consistent with our experiment results. It is beneficial to the application in the field of flexible photovoltaic spintronics. Actually, the underlying mechanism that the photo-magnetic effect can be larger under bent state is complex, and the discussion of this part is available in Supplementary Material for a preliminary understanding.

In addition, the good reversibility of magnetism has been investigated. The reversible switching of H_r can correspond to a two logic state switching, which may achieve future tunable flexible memories (more details are available in Supplementary Material). Fig. 3a shows the maximal ΔH_r shifting from 6736 to 6508 Oe under visible light (1 sun) with $1/r = 0$ mm^{-1} (flat condition), when the angle between the H-field and the Py membrane is 80°. After light illumination, H_r returns to 6735 Oe, implying good reversibility. Similarly, H_r locates from 6733 to 6452 Oe when applying 1 sun irradiation, then back to 6730 Oe when turning off the light with $1/r = 0.02$ mm^{-1} (bent condition), as shown in Fig. 3b. The $H_{r,OP}$ and the $H_{r,IP}$ with bending radius $1/r = 0.02$ mm^{-1} as a function of the light intensity (from 0 to 1.4 sun) is depicted in Fig. 3c. It can be seen that the $H_{r,OP}$ and $H_{r,IP}$ are changing inversely as the excitation light intensity ranges from 0 to 1.4 sun, which confirms that higher sunlight power triggers a weaker magnetic anisotropy. It means that more photo-induced electrons are doped into the Py layer to depress magnetism. To more accurately explain the sunlight illumination dependence of FMR field anisotropy, here, the magnetic anisotropy (H_a) could be quantitatively calculated and expressed as $H_a = H_{r,OP} - H_{r,IP}$. Fig. 3c illustrates the H_a with bending radius $1/r = 0.02$ mm^{-1} varies with the sunlight intensity. As the light intensity increases from 0 to 1.4 sun, H_a decreases from 5568 to 5025 Oe.

In summary, growing sunlight illumination shrinks the magnetic anisotropy of Py layer, evidenced by space magnetic anisotropy information. Furthermore, a *in situ* VSM is utilized to investigate the magnetic property change of magnetization of Py under bending, as shown in Fig. 3d. The ΔM_s is defined as $\Delta M_s = M_{s,1.4sun} - M_{s,dark} = -72$ emu/cm^3, where $M_{s,dark} = 548$ emu/cm^3 represents M_s before illumination, and $M_{s,1.4sun} = 476$ emu/cm^3 is M_s under visible light illumination. The

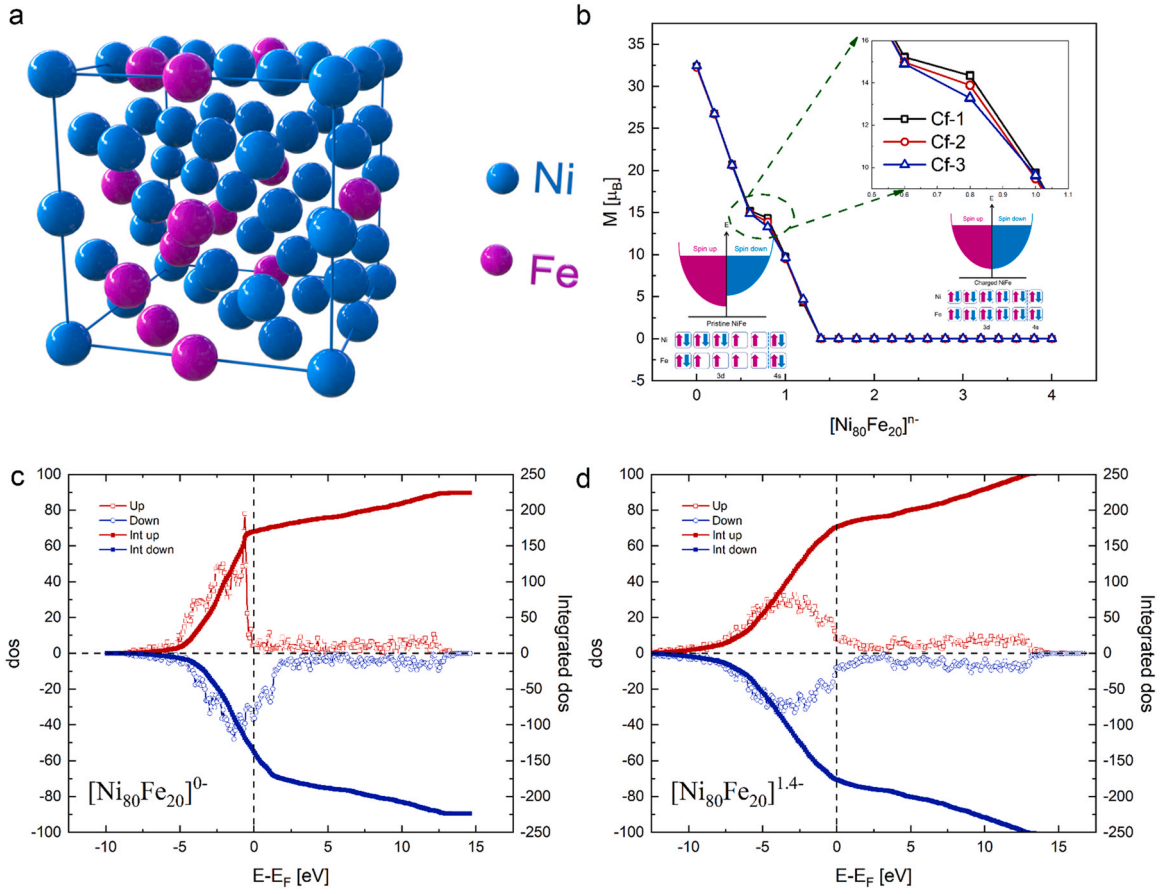

Fig. 4. Mechanisms of the photovoltaic control of magnetism. (a) The sketch of the calculated model. (b) The magnetizations *versus* photoelectrons of three independent random configurations. The spin resolved density of states for (c) n = 0 and (d) n = 1.4, respectively. "Int up" and "Int down" mean the integral of the density of the spin-up state and density of the spin-down state.

ΔM_s is approximately − 13.14% with light irradiation compared with the initial state without light, consistent with the ESR measurement.

To clarify this issue in Py films, we carried out the first-principles calculations using the Vienna *ab initio* simulation package (VASP). And for better performance on magnetism, the generalized-gradient-approximation (GGA) with an interpolation formula, according to Vosko, Wilk, and Nusair, are employed [44]. Furthermore, as the Py is an alloy, we set up a 2 × 2 × 2 supercell (32 atoms), as shown in Fig. 4a, and randomly put Ni and Fe atoms inside every position with equal possibilities to simulate an alloy of $Ni_{80}Fe_{20}$. Moreover, we choose the cutoff energy for the basis as 500 eV, and the convergence criterion for the electron density self-consistency cycles as 10^{-6} eV to converge the output. In the Brillouin zone, (5 × 5 × 5) k-point grids are sampled using the Monkhorst-Pack scheme [45].

The calculated magnetization of Py *versus* photoelectrons is plotted in Fig. 4b. We use 3 configurations of the Py to confirm our approximation on the construction of the calculated structures. All 3 configurations follow a similar tendency and closed values, and the magnetizations of Py decrease with increasing the injected electrons (n) and become nonmagnetic until n ≈ 1.4. For a better view of the changing when injecting electrons, we show the state density with n = 0 and n = 1.4 in Fig. 4c and d, respectively. We can see that, without photoelectrons, the unpaired electrons inside the 3d band of Ni ($3d^8 4s^2$) and Fe ($3d^6 4s^2$) lead to the unbalanced spin density, as shown in Fig. 4c. However, when n = 1.4, the extra photoelectrons fill in the empty d bands in Py and pull the spin up and spin down to equivalent energy levels. This is why it does not need to fill all the d bands in Py to vanish the magnetization, which would happen with n = 2.38 (n = 2 for Ni and n = 4 for Fe).

The possible interface coupling effect between the organic layer and the Py film as well as the thermal effect under the sunlight illumination needs to be excluded [46,47]. Fig. S3 shows a comparison between the Py film and Py/($PC_{71}BM$: PTB7-Th) film. The spin interface effect can be excluded because of no significant difference in H_r. Furthermore, the control experiment is conducted for the evaluation of the thermal effect. The magnetic anisotropy of PET/Ta/Py/Pt is *in situ* tested with $1/r = 0.02$ mm^{-1} under 1 sun illumination. As shown in Fig. S4, an apparent distinct tendency of the H_r shifts induced by the thermal effect and photovoltaic effect is observed respectively, suggesting that the light irradiation dominates the magnetic anisotropy manipulation process.

We can understand the whole optical gating process in the following steps. Step 1: The light response layer is excited by visible light to produce excitons. The excitons move around because of the diffusion effect. Step 2: When excitons spread to the interface of the donor and the acceptor, electrons and holes are separated and transferred to the photovoltaic layer——adjacent metal layer interface, which is driven by a built-in electrical field established by light induced charge carriers' concentration gradient. Step 3: Electrons move toward the magnetic layer and holes accumulate in the nonmagnetic layer due to an external electric field resulting from the difference of the work function among the electrodes (Pt= −5.65eV [48], Py= −5.25eV calculated in the Supplementary Material) where electrons are collected by lower work function metal while holes are collected by higher work function metal [49]. The Fermi Level of the Py is altered with the injected electrons filling the orbital, thus the magnetic anisotropy is weakened. Step 4: After the light source is switched off, the recombination process of electron-hole pairs is

dominated, and then the magnetic anisotropy change is switched back.

3. Conclusions

Consequently, a precisely controllable photovoltaic flexible spintronics device has been demonstrated with the structure of PET/Ta/Py/organic active layer/Pt. About 281 Oe of maximal FMR shift was achieved reversibly for the deformed device with a bending radius of 50 mm at RT. Besides, the increasing sunlight decreased the H_a. Meanwhile, the first-principles calculation was also conducted further to reveal the mechanism of photovoltaic control of ferromagnetism. With high tunability, excellent controllability, flexibility, conformity and deformation stability, the photovoltaic flexible spintronics device provides a platform capable of magnetic sensors, and a tunable electronic device based on which wearable electrics for navigation, and medical diagnosis, high-frequency microwave device, and health monitoring can be realized.

4. Experimental section

4.1. Device fabrication

We chose 100 μm thick PET foils (DuPont, US) as the flexible substrate for its low price, good mechanical properties, excellent chemical resistance, high transparency, avirulence and compatible with roll-to-roll processing. And then 4 nm Ta films (seed layers) and 1.7 nm Py were deposited onto the PET substrates in turn *via* DC magnetron sputtering. The film thickness was controlled with a quartz crystal microbalance integrated into a magnetron sputtering system, and no further *in situ* annealing was performed. The organic semiconductor layer ($PC_{71}BM$: PTB7-Th) was spin-coated onto Py film without any surface treatment to form a bulk heterojunction structure as a photovoltaic layer, where PTB7-Th was used as the donor and $PC_{71}BM$ as the acceptor. PTB7-Th and $PC_{71}BM$ were purchased from 1-Material Chemscitech Inc. (Canada). In detail, PTB7-Th and $PC_{71}BM$ (ratio 1:1.5) were dissolved in the halogen-free solvent (oxylene) with 3% (volume fraction) of 1,8-diiodooctane (DIO) and stirred overnight, with a polymer concentration of 8 mg/mL. The solutions were coated onto the as-grown ferromagnetic film at 2000 rpm in an ambient atmosphere to obtain approximately 50–60 nm thickness. A 3 nm semitransparent Pt film was then deposited on the $PC_{71}BM$/PTB7-Th light respond layer as a top electrode by DC magnetron sputtering.

4.2. In situ magnetic measurement

The *in situ* ESR measurement was conducted with a JEOL FA200 ESR system. The device was characterized in a TE 011 mode microwave cavity. The *in situ* VSM measurement was carried out in a LakeShore 7404 VSM system. The simulated sunlight was supplied with a Xenon Lamp House (HSX-F300, NBeT Co. Beijing, China) with an Ultraviolet filter, and the light intensity on the sample was corrected with an irradiance meter before the *in situ* measurement.

CRediT authorship contribution statement

Wanjun Peng: Writing – original draft, Investigation, Formal analysis. **Lei Wang:** Formal analysis, Writing – review & editing. **Yaojin Li:** Formal analysis. **Yujing Du:** Investigation. **Zhexi He:** Investigation. **Chenying Wang:** Validation. **Yifan Zhao:** Conceptualization, Writing – review & editing. **Zhuangde Jiang:** Resources, Supervision. **Ziyao Zhou:** Resources, Writing – review & editing, Supervision. **Ming Liu:** Resources, Supervision, Project administration.

Declaration of Competing Interest

The authors declare that they have no known competing financial interests or personal relationships that could have appeared to influence the work reported in this paper.

Acknowledgments

This work was supported by the National Natural Science Foundation of China (No.52175434, 52172126, 62001366, 91964109, 11804266 and 11534015), the National Key R & D Program of China (2018YFB0407601, 2019YFA0307900), and the Fundamental Research Funds for the Central Universities (xjh012019042), and the National 111 Project of China (B14040), and the China Postdoctoral Science Foundation (No. 2021T140549).

Appendix A. Supporting information

Supplementary data associated with this article can be found in the online version at doi:10.1016/j.jallcom.2022.164903.

References

[1] Q. Yang, Z.Y. Zhou, L.Q. Wang, H.J. Zhang, Y.X. Cheng, Z.Q. Hu, B. Peng, M. Liu, Ionic gel modulation of RKKY interactions in synthetic anti-ferromagnetic nanostructures for low power wearable spintronic devices, Adv. Mater. 30 (2018) 1800449.
[2] Z.G. Wang, X.J. Wang, M.H. Li, Y. Gao, Z.Q. Hu, T.X. Nan, X.F. Liang, H.H. Chen, J. Yang, S. Cash, N.X. Sun, Highly sensitive flexible magnetic sensor based on anisotropic magnetoresistance effect, Adv. Mater. 28 (2016) 9370–9377.
[3] M.K. Mohanta, I.S. Fathima, A. Kishore, A. De Sarkar, Spin-current modulation in hexagonal buckled ZnTe and CdTe monolayers for self-powered flexible-piezo-spintronic devices, ACS Appl. Mater. Interfaces 13 (2021) 40872–40879.
[4] S. Ota, A. Ando, D. Chiba, A flexible giant magnetoresistive device for sensing strain direction, Nat. Electron. 1 (2018) 124–129.
[5] Y.N. Zhao, R.C. Peng, Y.T. Guo, Z.J. Liu, Y.Q. Dong, S.S. Zhao, Y.J. Li, G.H. Dong, Y. Hu, J.W. Zhang, Y. Peng, T.N. Yang, B. Tian, Y.F. Zhao, Z.Y. Zhou, Z.D. Jiang, Z.L. Luo, M. Liu, Ultraflexible and malleable Fe/BaTiO3 multiferroic heterostructures for functional devices, Adv. Funct. Mater. 31 (2021) 2009376.
[6] D.M. Sun, M.Y. Timmermans, Y. Tian, A.G. Nasibulin, E.I. Kauppinen, S. Kishimoto, T. Mizutani, Y. Ohno, Flexible high-performance carbon nanotube integrated circuits, Nat. Nanotechnol. 6 (2011) 156–161.
[7] J.F. Sierra, J. Fabian, R.K. Kawakami, S. Roche, S.O. Valenzuela, Van der Waals heterostructures for spintronics and opto-spintronics, Nat. Nanotechnol. 16 (2021) 856–868.
[8] I.G. Serrano, J. Panda, F. Denoel, O. Vallin, D. Phuyal, O. Karis, M.V. Kamalakar, Two-dimensional flexible high diffusive spin circuits, Nano Lett. 19 (2019) 666–673.
[9] S.R. Forrest, The path to ubiquitous and low-cost organic electronic appliances on plastic, Nature 428 (2004) 911–918.
[10] C.Y. Hung, M. Mao, S. Funada, T. Schneider, L. Miloslavsky, M. Miller, C. Qian, H.C. Tong, Magnetic properties of ultrathin NiFe and CoFe films, J. Appl. Phys. 87 (2000) 6618–6620.
[11] J. Singh, S.K. Gupta, A.K. Singh, P. Kothari, R.K. Kotnala, J. Akhtar, Investigation of structural and magnetic properties of Ni, NiFe and $NiFe_2O_4$ thin films, J. Magn. Magn. Mater. 324 (2012) 999–1005.
[12] Z.Q. Hu, X.J. Wang, T.X. Nan, Z.Y. Zhou, B.H. Ma, X.Q. Chen, J.G. Jones, B.M. Howe, G.J. Brown, Y. Gao, H. Lin, Z.G. Wang, R.D. Guo, S.Y. Chen, X.L. Shi, W. Shi, H.Z. Sun, D. Budil, M. Liu, N.X. Sun, Non-volatile ferroelectric switching of ferromagnetic resonance in NiFe/PLZT multiferroic thin film heterostructures, Sci. Rep. 6 (2016) 32408.
[13] F. Matsukura, Y. Tokura, H. Ohno, Control of magnetism by electric fields, Nat. Nanotechnol. 10 (2015) 209–220.
[14] S.S. Zhao, L. Wang, Z.Y. Zhou, C.L. Li, G.H. Dong, L. Zhang, B. Peng, T. Min, Z.Q. Hu, J. Ma, W. Ren, Z.G. Ye, W. Chen, P. Yu, C.W. Nan, M. Liu, Ionic liquid gating control of spin reorientation transition and switching of perpendicular magnetic anisotropy, Adv. Mater. 30 (2018) 1801639.
[15] A.V. Kimel, M. Li, Writing magnetic memory with ultrashort light pulses, Nat. Rev. Mater. 4 (2019) 189–200.
[16] C.H. Lambert, S. Mangin, B.S.D.CH.S. Varaprasad, Y.K. Takahashi, M. Hehn, M. Cinchetti, G. Malinowski, K. Hono, Y. Fainman, M. Aeschlimann, E.E. Fullerton, All-optical control of ferromagnetic thin films and nanostructures, Science 345 (2014) 1337–1340.
[17] Y.J. Du, S.P. Wang, L. Wang, S.Y. Jin, Y.F. Zhao, T. Min, Z.D. Jiang, Z.Y. Zhou, M. Liu, Improving solar control of magnetism in ternary organic photovoltaic system with enhanced photo-induced electrons doping, Nano Res. (2021).
[18] Y.F. Chen, Y.F. Mei, R. Kaltofen, J.I. Monch, J. Schumann, J. Freudenberger, H.J. Klauss, O.G. Schmidt, Towards flexible magnetoelectronics: Buffer-enhanced

and mechanically tunable GMR of Co/Cu multilayers on plastic substrates, Adv. Mater. 20 (2008) 3224–3228.
[19] N. Perez, M. Melzer, D. Makarov, O. Ueberschar, R. Ecke, S.E. Schulz, O.G. Schmidt, High-performance giant magnetoresistive sensorics on flexible Si membranes, Appl. Phys. Lett. 106 (2015) 153501.
[20] C.Y. Wang, H.J. Zhang, C.L. Li, Y. He, L. Zhang, X.E. Zhao, Q. Yang, D. Xian, Q. Mao, B. Peng, Z.Y. Zhou, W.Z. Cui, Z.Q. Hu, Voltage control of magnetic anisotropy through ionic gel gating for flexible spintronics, ACS Appl. Mater. Interfaces 10 (2018) 29750–29756.
[21] G.S. Huang, Y.F. Mei, Thinning and shaping solid films into functional and integrative nanomembranes, Adv. Mater. 24 (2012) 2517–2546.
[22] T. Brintlinger, S.H. Lim, K.H. Baloch, P. Alexander, Y. Qi, J. Barry, J. Melngailis, L. Salamanca-Riba, I. Takeuchi, J. Cumings, In situ observation of reversible nanomagnetic switching induced by electric fields, Nano Lett. 10 (2010) 1219–1223.
[23] G.H. Dong, Z.Y. Zhou, X. Xue, Y.J. Zhang, B. Peng, M.M. Guan, S.S. Zhao, Z.Q. Hu, W. Ren, Z.G. Ye, M. Liu, Ferroelectric phase transition induced a large FMR tuning in self assembled $BaTiO_3$:$Y_3Fe_5O_{12}$ multiferroic composites, ACS Appl. Mater. Interfaces 9 (2017) 30733–30740.
[24] L. Wang, X.R. Wang, T. Min, K. Xia, Charge-induced ferromagnetic phase transition and anomalous Hall effect in full d-band nonmagnetic metals, Phys. Rev. B 99 (2019) 224416.
[25] L. Tan, L. Wang, T. Min, Tunable magnetic ground states of iron monolayer on nonmagnetic metallic substrates by small in-plane strains, RSC Adv. 9 (2019) 41099–41106.
[26] C.C. Chiang, S.Y. Huang, D. Qu, P.H. Wu, C.L. Chien, Absence of evidence of electrical switching of the antiferromagnetic Neel vector, Phys. Rev. Lett. 123 (2019) 227203.
[27] N.A. Spaldin, R. Ramesh, Advances in magnetoelectric multiferroics, Nat. Mater. 18 (2019) 203–212.
[28] S. Manipatruni, D.E. Nikonov, C.C. Lin, T.A. Gosavi, H.C. Liu, B. Prasad, Y.L. Huang, E. Bonturim, R. Ramesh, I.A. Young, Scalable energy-efficient magnetoelectric spin-orbit logic, Nature 565 (2019) 35–42.
[29] L. Caretta, M. Mann, F. Buttner, K. Ueda, B. Pfau, C.M. Gunther, P. Hessing, A. Churikoval, C. Klose, M. Schneider, D. Engel, C. Marcus, D. Bono, K. Bagschik, S. Eisebitt, G.S.D. Beach, Fast current-driven domain walls and small skyrmions in a compensated ferrimagnet, Nat. Nanotechnol. 13 (2018) 1154–1160.
[30] N.P. Lu, P.F. Zhang, Q.H. Zhang, R.M. Qiao, Q. He, H.B. Li, Y.J. Wang, J.W. Guo, D. Zhang, Z. Duan, Z.L. Li, M. Wang, S.Z. Yang, M.Z. Yan, E. Arenholz, S.Y. Zhou, W.L. Yang, L. Gu, C.W. Nan, J. Wu, Y. Tokura, P. Yu, Electric-field control of tri-state phase transformation with a selective dual-ion switch, Nature 546 (2017) 124–128.
[31] Y. Ba, S.A. Zhuang, Y.K. Zhang, Y.T. Wang, Y. Gao, H.A. Zhou, M.F. Chen, W.D. Sun, Q. Liu, G.Z. Chai, J. Ma, Y. Zhang, H.F. Tian, H.F. Du, W.J. Jiang, C.W. Nan, J.M. Hu, Y.G. Zhao, Electric-field control of skyrmions in multiferroic heterostructure via magnetoelectric coupling, Nat. Commun. 12 (2021) 322.
[32] X.Z. Chen, S.Y. Shi, G.Y. Shi, X.L. Fan, C. Song, X.F. Zhou, H. Bai, L.Y. Liao, Y.J. Zhou, H.W. Zhang, A. Li, Y.H. Chen, X.D. Han, S. Jiang, Z.W. Zhu, H.Q. Wu, X.R. Wang, D.S. Xue, H. Yang, F. Pan, Observation of the antiferromagnetic spin Hall effect, Nat. Mater. 20 (2021) 800–804.
[33] Z.Q. Liu, H. Chen, J.M. Wang, J.H. Liu, K. Wang, Z.X. Feng, H. Yan, X.R. Wang, C.B. Jiang, J.M.D. Coey, A.H. MacDonald, Electrical switching of the topological anomalous Hall effect in a non-collinear antiferromagnet above room temperature, Nat. Electron. 1 (2018) 172–177.
[34] S.D. Li, G.X. Miao, D.R. Cao, Q. Li, J. Xu, Z. Wen, Y.Y. Da, S.S. Yan, Y.G. Lu, Stress-enhanced interlayer exchange coupling and optical-mode FMR frequency in self-bias FeCoB/Ru/FeCoB trilayers, ACS Appl. Mater. Interfaces 10 (2018) 8853–8859.
[35] C.Y. Guo, C.H. Wan, W.Q. He, M.K. Zhao, Z.R. Yan, Y.W. Xing, X. Wang, P. Tang, Y.Z. Liu, S. Zhang, Y.W. Liu, X.F. Han, A nonlocal spin Hall magnetoresistance in a platinum layer deposited on a magnon junction, Nat. Electron. 3 (2020) 304–308.
[36] Y.D. Liou, S.Z. Ho, W.Y. Tzeng, Y.C. Liu, P.C. Wu, J.D. Zheng, R. Huang, C.G. Duan, C.Y. Kuo, C.W. Luo, Y.C. Chen, J.C. Yang, Extremely fast optical and nonvolatile control of mixed-phase multiferroic BiFeO3 via instantaneous strain perturbation, Adv. Mater. 33 (2021) 2007264.
[37] Y.C. Guan, X.L. Zhou, T.P. Ma, R. Blasing, H. Deniz, S.H. Yang, S.S.P. Parkin, Increased efficiency of current-induced motion of chiral domain walls by interface engineering, Adv. Mater. 33 (2021) 2007991.
[38] Y.F. Zhao, S.S. Zhao, L. Wang, Z.Y. Zhou, J.X. Liu, T. Min, B. Peng, Z.Q. Hu, S.Y. Jin, M. Liu, Sunlight control of interfacial magnetism for solar driven spintronic applications, Adv. Sci. 6 (2019) 1901994.
[39] S.H. Liao, H.J. Jhuo, Y.S. Cheng, S.A. Chen, Fullerene derivative-doped zinc oxide nanofilm as the cathode of inverted polymer solar cells with low-bandgap polymer (PTB7-Th) for high performance, Adv. Mater. 25 (2013) 4766–4771.
[40] J.M. Hu, L.Q. Chen, C.W. Nan, Multiferroic heterostructures integrating ferroelectric and magnetic materials, Adv. Mater. 28 (2016) 15–39.
[41] M. Liu, B.M. Howe, L. Grazulis, K. Mahalingam, T.X. Nan, N.X. Sun, G.J. Brown, Voltage-impulse-induced non-volatile ferroelastic switching of ferromagnetic resonance for reconfigurable magnetoelectric microwave devices, Adv. Mater. 25 (2013) 4886–4892.
[42] M. Liu, Z.Y. Zhou, T.X. Nan, B.M. Howe, G.J. Brown, N.X. Sun, Voltage tuning of ferromagnetic resonance with bistable magnetization switching in energy-efficient magnetoelectric composites, Adv. Mater. 25 (2013) 1435–1439.
[43] S.S. Zhao, Z.Y. Zhou, C.L. Li, B. Peng, Z.Q. Hu, M. Liu, Low-voltage control of (Co/Pt)(X) perpendicular magnetic anisotropy heterostructure for flexible spintronics, ACS Nano 12 (2018) 7167–7173.
[44] S.H. Vosko, L. Wilk, M. Nusair, Accurate spin-dependent electron liquid correlation energies for local spin-density calculations - a critical analysis, Can. J. Phys. 58 (1980) 1200–1211.
[45] H.J. Monkhorst, J.D. Pack, Special points for Brillouin-Zone integrations, Phys. Rev. B 13 (1976) 5188–5192.
[46] K.V. Raman, A.M. Kamerbeek, A. Mukherjee, N. Atodiresei, T.K. Sen, P. Lazic, V. Caciuc, R. Michel, D. Stalke, S.K. Mandal, S. Blugel, M. Munzenberg, J.S. Moodera, Interface-engineered templates for molecular spin memory devices, Nature 493 (2013) 509–513.
[47] Y.F. Zhao, S.S. Zhao, L. Wang, S.P. Wang, Y.J. Du, Y.A. Zhao, S.Y. Jin, T. Min, B. Tian, Z.D. Jiang, Z.Y. Zhou, M. Liu, Photovoltaic modulation of ferromagnetism within a FM metal/P-N junction Si heterostructure, Nanoscale 13 (2021) 272–279.
[48] Y.F. Zhao, M. Zhao, B. Tian, Z.D. Jiang, Y.H. Wang, M. Liu, Z.Y. Zhou, Enhancing sunlight control of interfacial magnetism by introducing the ZnO layer for electron harvesting, ACS Appl. Mater. Interfaces 13 (2021) 2018–2024.
[49] V. Coropceanu, J. Cornil, D.A. da Silva, Y. Olivier, R. Silbey, J.L. Bredas, Charge transport in organic semiconductors, Chem. Rev. 107 (2007) 926–952.